Ultra-Strongly Self-Interacting Dark Matter: From Phenomenology to Observables

M. Grant Roberts

Co-Authors: Pierce Giffin, Stefano Profumo, Wolfgang Altmannshofer
Email: migrober@ucsc.edu

Physics
UC Santa Cruz

October 23, 2025

Introduction

From papers:

- Early formation of supermassive black holes from the collapse of strongly self-interacting dark matter (arXiv:2410.17480 → JCAP)
- Little Red Dots from Ultra-Strongly Self-Interacting Dark Matter (arXiv:2507.03230 → responding to referee JCAP)
- Ultra-Strongly Self-Interacting Dark Matter: From Phenomenology to Astrophysical Observables (arXiv:2510.18142)

Basic outline of the topics that will be presented:

- Motivation of why SIDM and uSIDM
- uSIDM Phenomenology
- Future works

Motivation of why SIDM and uSIDM

Why SIDM?

- SIDM solves small scale structure problems: Core-cusp, diversity of rotation curves, and too-big-too-fail

Why uSIDM?

- uSIDM collapses the inner DM halo core into BH seeds, which can grow to the observed high-z quasar measurements

Little Red Dots from uSIDM

LRDs are a newly observed class of compact, high redshift ($z \gtrsim 5$) AGN that may be $> 10\times$ more numerous than quasars. Images taken from Kocevski et al 2024 arXiv:2404.03576

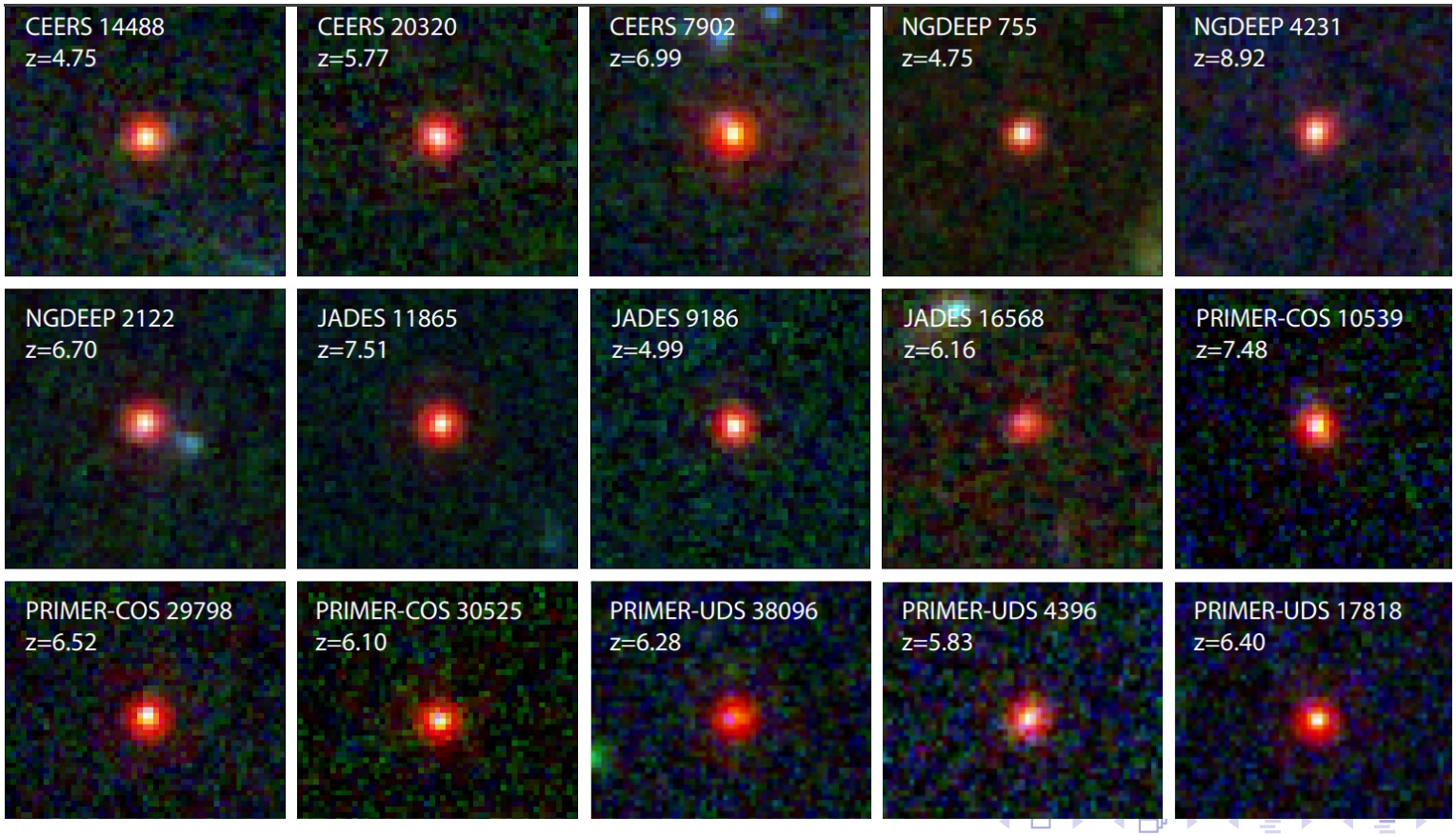

LRD Mass Function from uSIDM

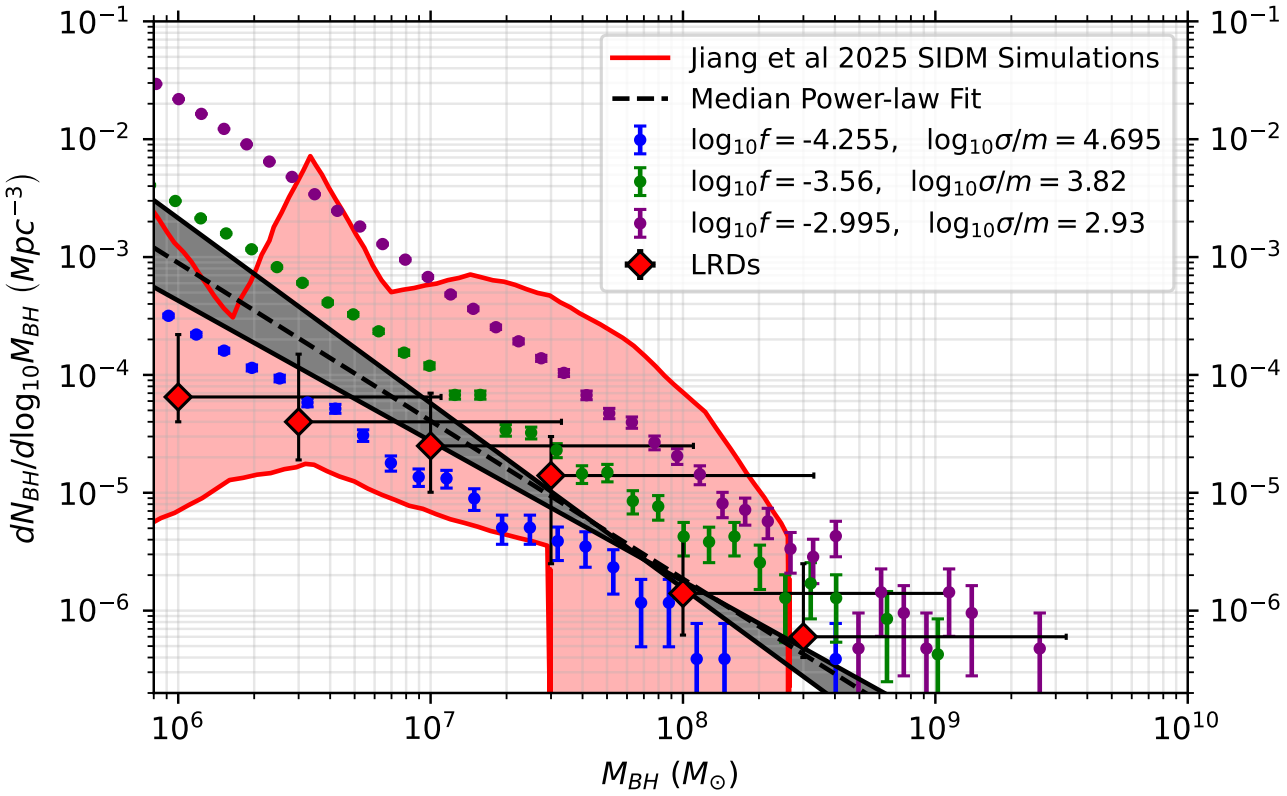

Figure: We show the uSIDM LRD mass function (colored dots) for different uSIDM parameters taken from Fig. 3 in Roberts et al 2025, arXiv:2507.03230, plotted against the SIDM simulation results from Jiang et al 2025, arXiv:2503.23710 (shaded red), and the LRD mass function data points from Kokorev et al 2024, arXiv:2401.09981 (red diamonds).

uSIDM Phenomenology

Can we have both SIDM and uSIDM?
→ How can this be constrained?
→ And what are the consequences?

uSIDM Phenomenology

- 2 DM particles:
  - χ_1 = uSIDM particle
  - χ_2 = regular SIDM particle
- 1 dark photon A'^{μ} (no kinetic mixing yet, will talk about that later)

$$\mathcal{L}_{\text{dark}} = \overline{\chi}_1 \left(i\partial\!\!\!/ - m_\chi\right) \chi_1 + \overline{\chi}_2 \left(i\partial\!\!\!/ - m_\chi\right) \chi_2 - g_{\chi_1} \overline{\chi}_1 A'^{\mu} \gamma_\mu \chi_1$$
$$- g_{\chi_2} \overline{\chi}_2 A'^{\mu} \gamma_\mu \chi_2 - \frac{1}{4} F'^{\mu\nu} F'_{\mu\nu} - \frac{1}{2} m_{A'}^2 A'^{\mu} A'_{\mu},$$

We also have the conditions that $m_{\chi_1} = m_{\chi_2}$, $g_{\chi_2} \sim g_{\chi_1} f^{1/4}$, and $f << 1$: so to specify the full model, we have 4 free parameters: $\left\{m_\chi,\ m_{A'},\ g_{\chi_1},\ f_{\text{uSIDM}}^{\text{initial}}\right\}$.

uSIDM Phenomenology

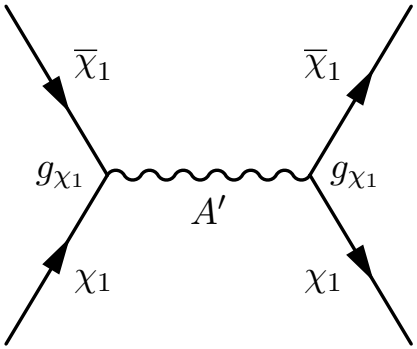

(a) Number-conserving

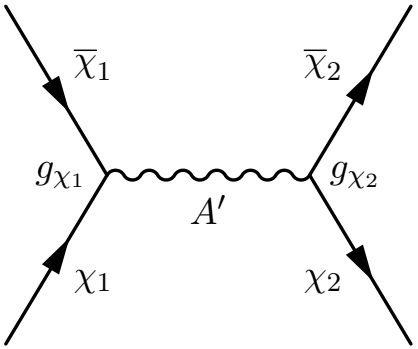

(b) Number-changing

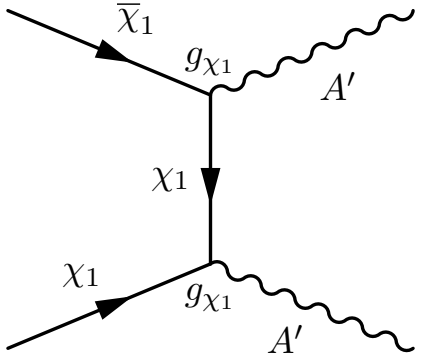

(c) $\chi_1\chi_1 \to A'A'$ (or $\chi_2\chi_2 \to A'A'$)

Figure: uSIDM $2 \to 2$ processes.

uSIDM Phenomenology

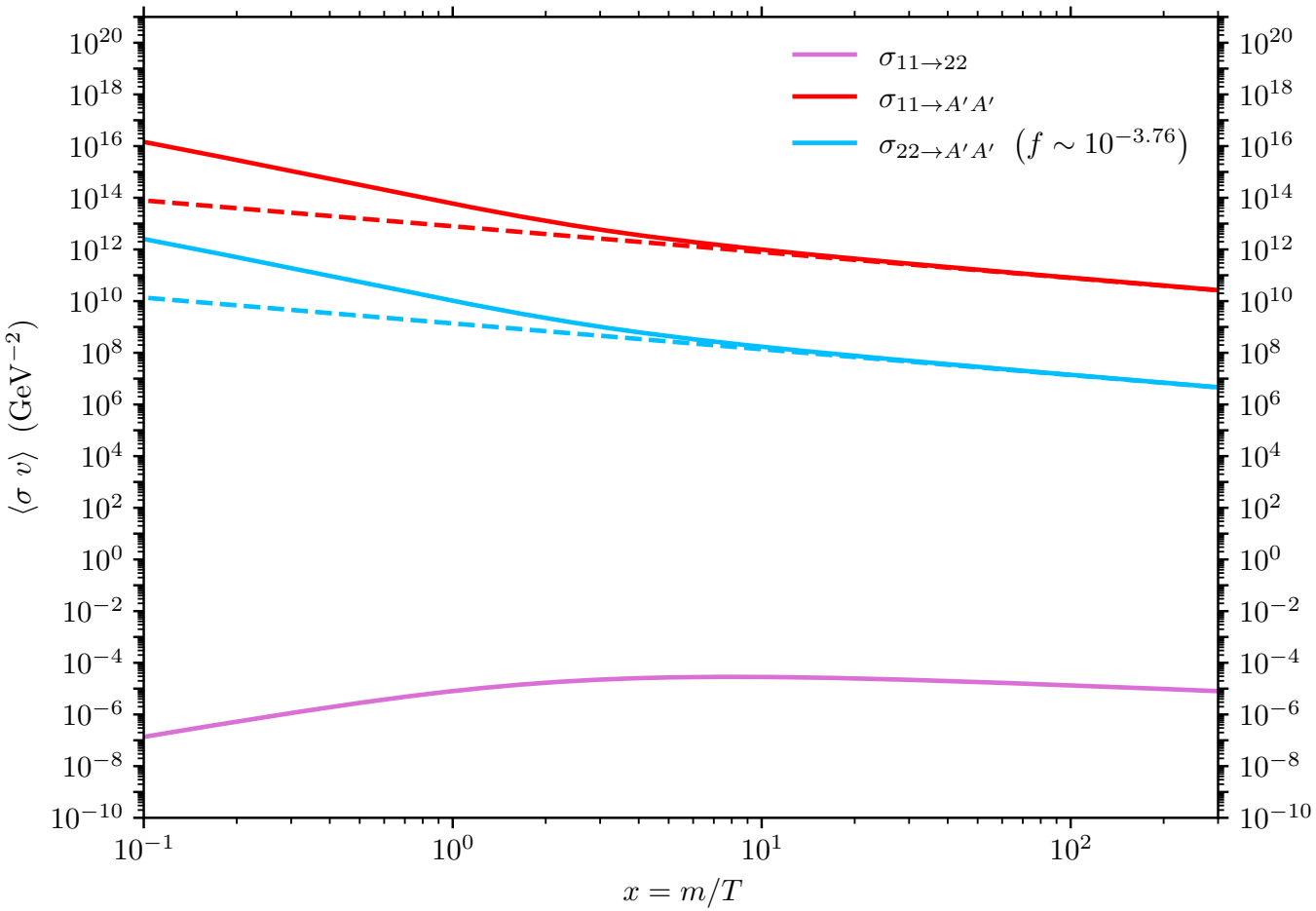

$$\frac{dY_1}{dx} = \frac{-s}{Hx}\left[\langle\sigma v\rangle_{11\longrightarrow A'A'}\left(Y_1^2 - Y_{1,eq}^2\right) + \langle\sigma v\rangle_{11\longrightarrow 22}\left(Y_1^2 - Y_2^2\right)\right]$$
$$\frac{dY_2}{dx} = \frac{-s}{Hx}\left[\langle\sigma v\rangle_{22\longrightarrow A'A'}\left(Y_2^2 - Y_{2,eq}^2\right) + \langle\sigma v\rangle_{11\longrightarrow 22}\left(Y_2^2 - Y_1^2\right)\right]$$

Because of this hierarchy of cross-sections, we are able to solve each Boltzmann equation analytically:

$$Y(\infty) \sim \frac{3.79\ x_f}{\sqrt{g^*} M_{\rm pl}\langle\sigma v\rangle_{11/22\longrightarrow A'A'}}$$
$$\Omega_\chi h^2 = \frac{h^2 m_\chi s_0 Y(\infty)}{\rho_{\rm crit}} \sim 2.742\times 10^8 m_\chi Y(\infty)$$
$$\longrightarrow \Omega_{\rm DM}{\rm h}^2 = \Omega_{\chi_1}h^2 + \Omega_{\chi_2}h^2$$
$$\longrightarrow f_{\rm uSIDM}^{\rm end} = \frac{\Omega_{\chi_1}h^2}{\Omega_{\chi_1}h^2 + \Omega_{\chi_2}h^2}$$

By expanding $< \sigma v >$, we can derive an analytic result for the relationship between $\alpha_\chi = \frac{g_\chi^2}{4\pi}$ and m_χ:

$$\longrightarrow \left(\frac{m_\chi}{\text{Gev}}\right) \sim \frac{\alpha_{\chi 2}}{4.96 \times 10^{-6}} \frac{1}{\sqrt{x_{f1} f + x_{f2}}}$$

$$\longrightarrow f_{\text{uSIDM}}^{\text{end}} \sim 10^{-3.5} \left(\frac{x_{f_1}}{30}\right) \left(\frac{20}{x_{f_2}}\right) \left(\frac{f_{\text{uSIDM}}^{\text{initial}}}{10^{-3.76}}\right)$$

i.e., the uSIDM particle only introduces a small correction onto the usual SIDM thermal relic relation. Now we have everything we need to constrain the uSIDM model with current observations.

Observational Constraints:

- SIDM cross-section measurements via rotation curves and strong cluster lensing
- Matter Power Spectrum
- Direct detection

uSIDM Observables: Rotation Curves/Strong Lensing

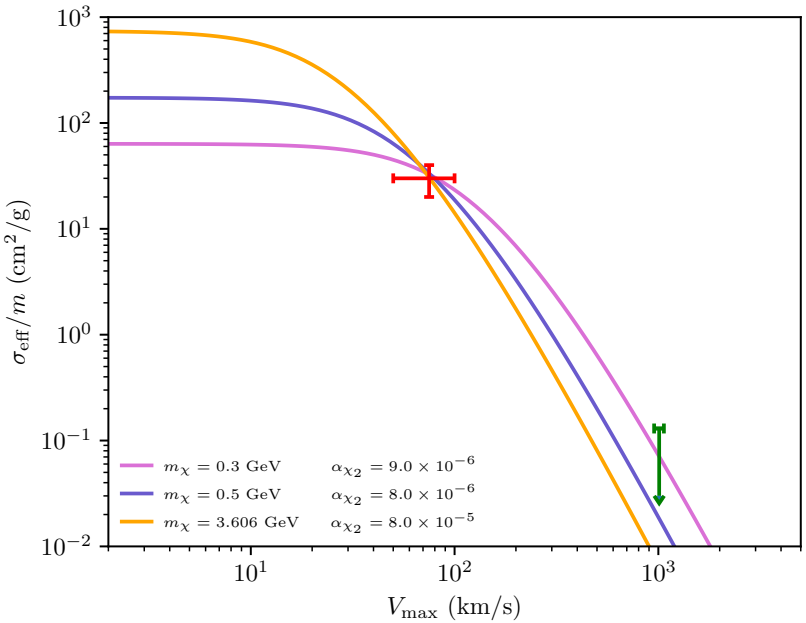

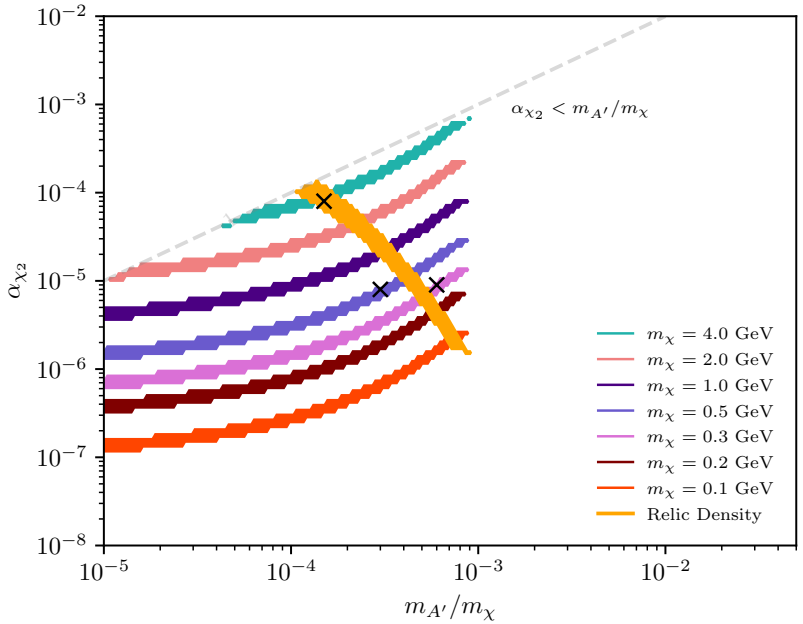

uSIDM Observables: Matter Power Spectrum

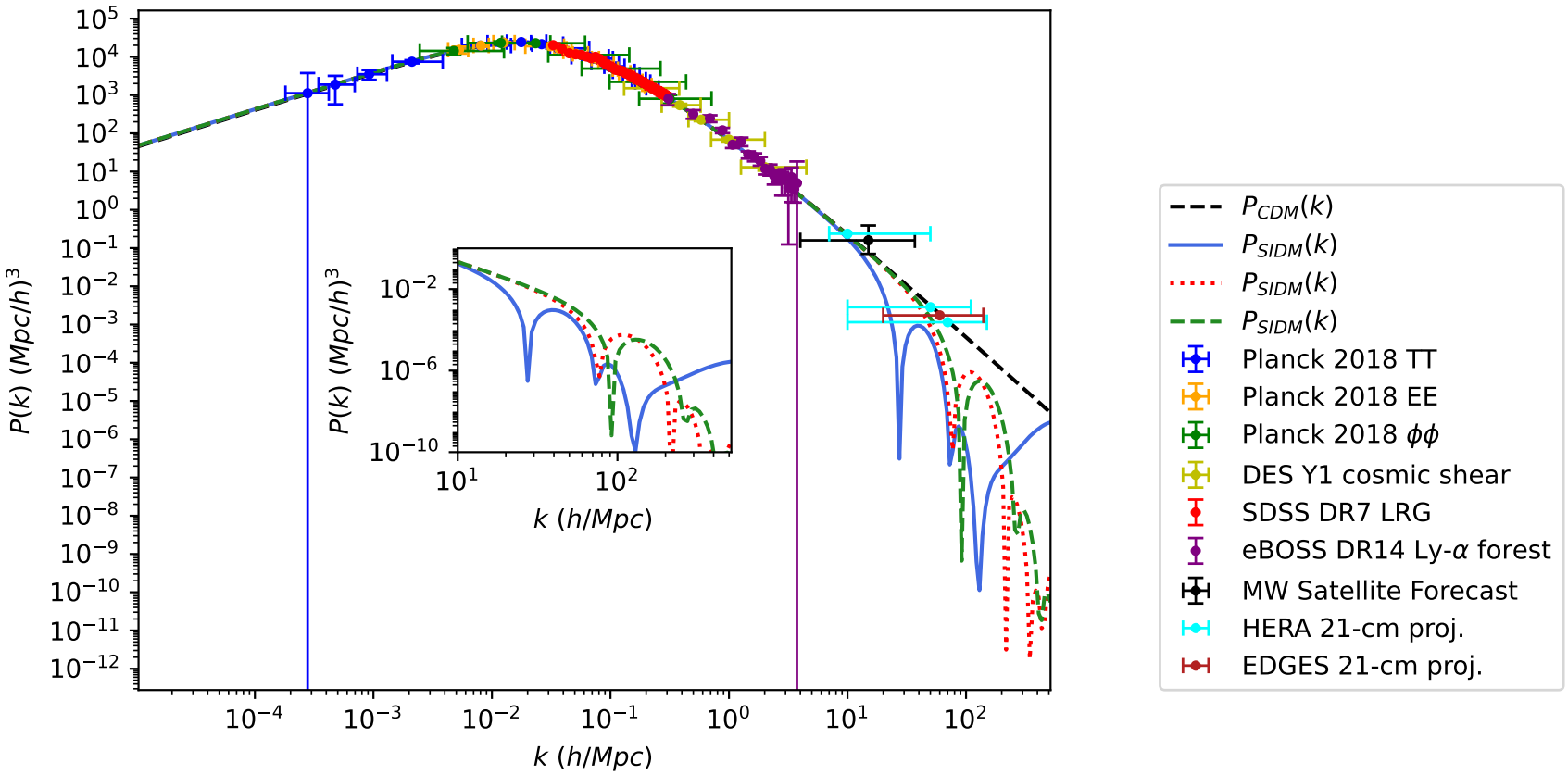

Figure: Example: the solid blue curve $m_{\chi_1} = 3.606$ GeV, $m_{A'} = 5.4 \times 10^{-4}$ GeV, $\alpha_{\chi_2} = 8 \times 10^{-5}$ - we plot the corresponding matter power spectrum.

uSIDM Observables: Direct Detection

If we turn on kinetic mixing, then we can look at nucleon recoil constraints. From supernova cooling, $\varepsilon_\gamma \lesssim 10^{-10}$:

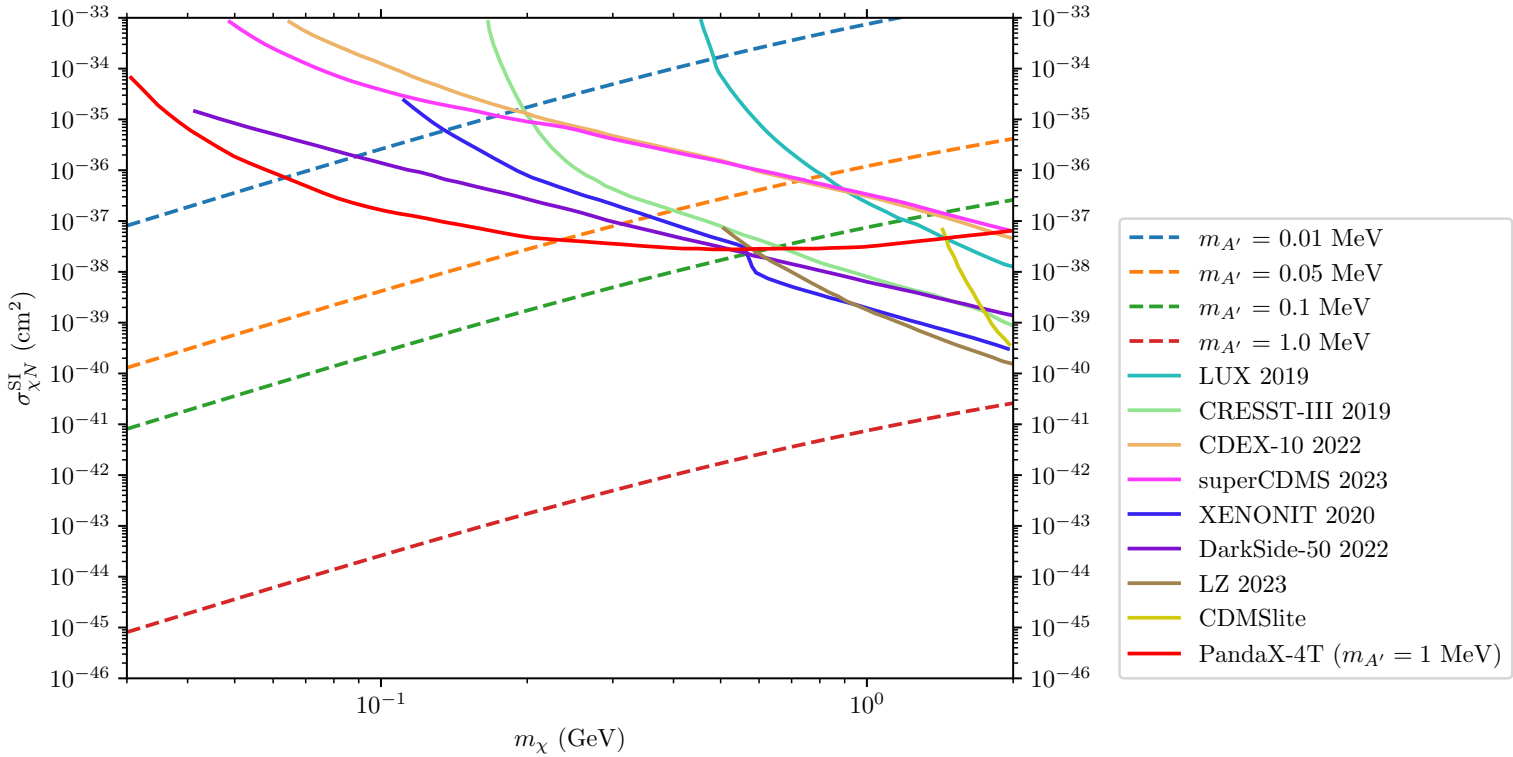

Figure: PandaX-4T experimental paper with other constraints: https://arxiv.org/pdf/2308.01540

uSIDM Observables: Direct Detection

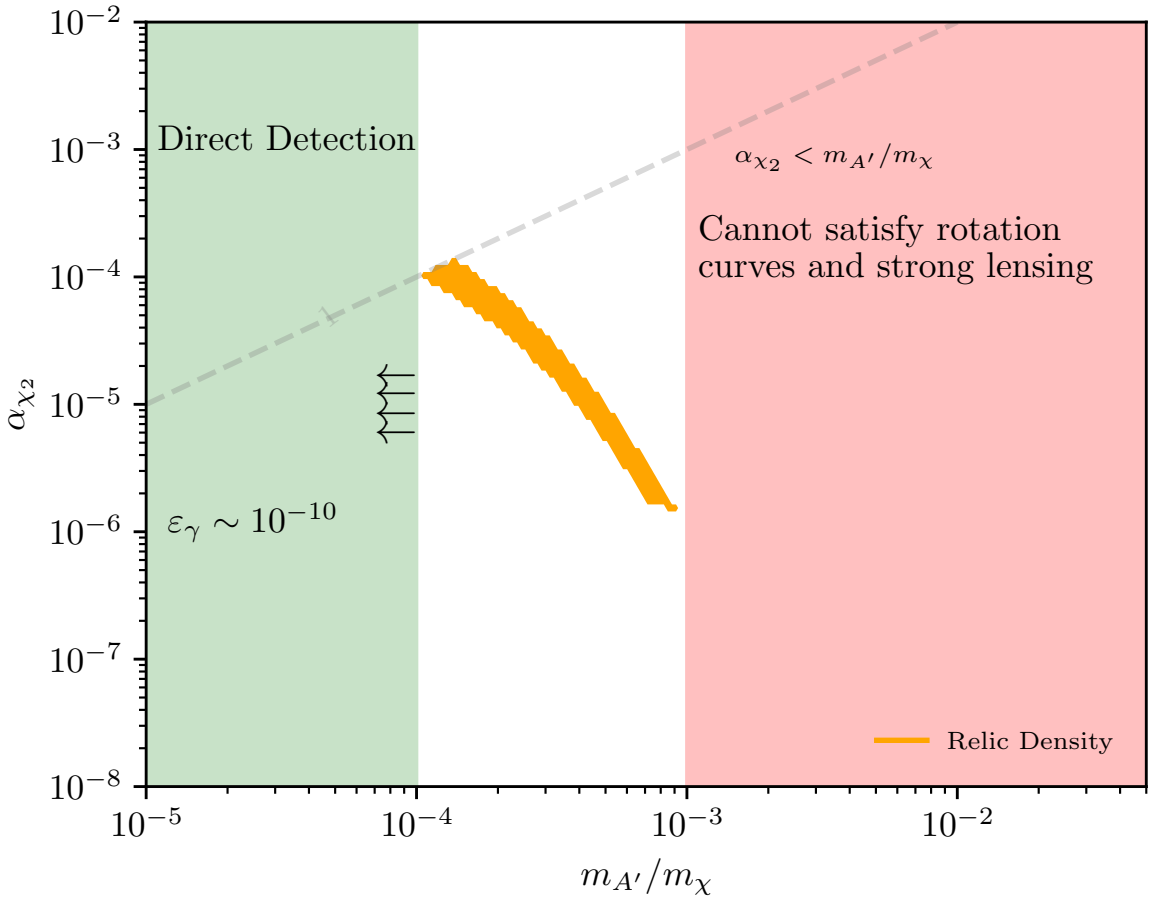

Figure: Green region: ruled out from direct detection searches. Red region: $w/c = m_{A'}/m_\chi \sim 10^{-3}$ represents the "bend" or transition region in the cross-section between the constant and $1/v^4$ region, so anything beyond the $10^{-3}c$ velocity scale will overshoot or undershoot

uSIDM in general

Future works:

- LRD clustering calculations
- Can the uSIDM model impact other LRD special features?
- Milky Way scale constraints on SIDM σ/m from uSIDM σ/m?

Conclusion

Thank you for listening, do you have any questions?

Backup Slides

SIDM and uSIDM cross-section comparison

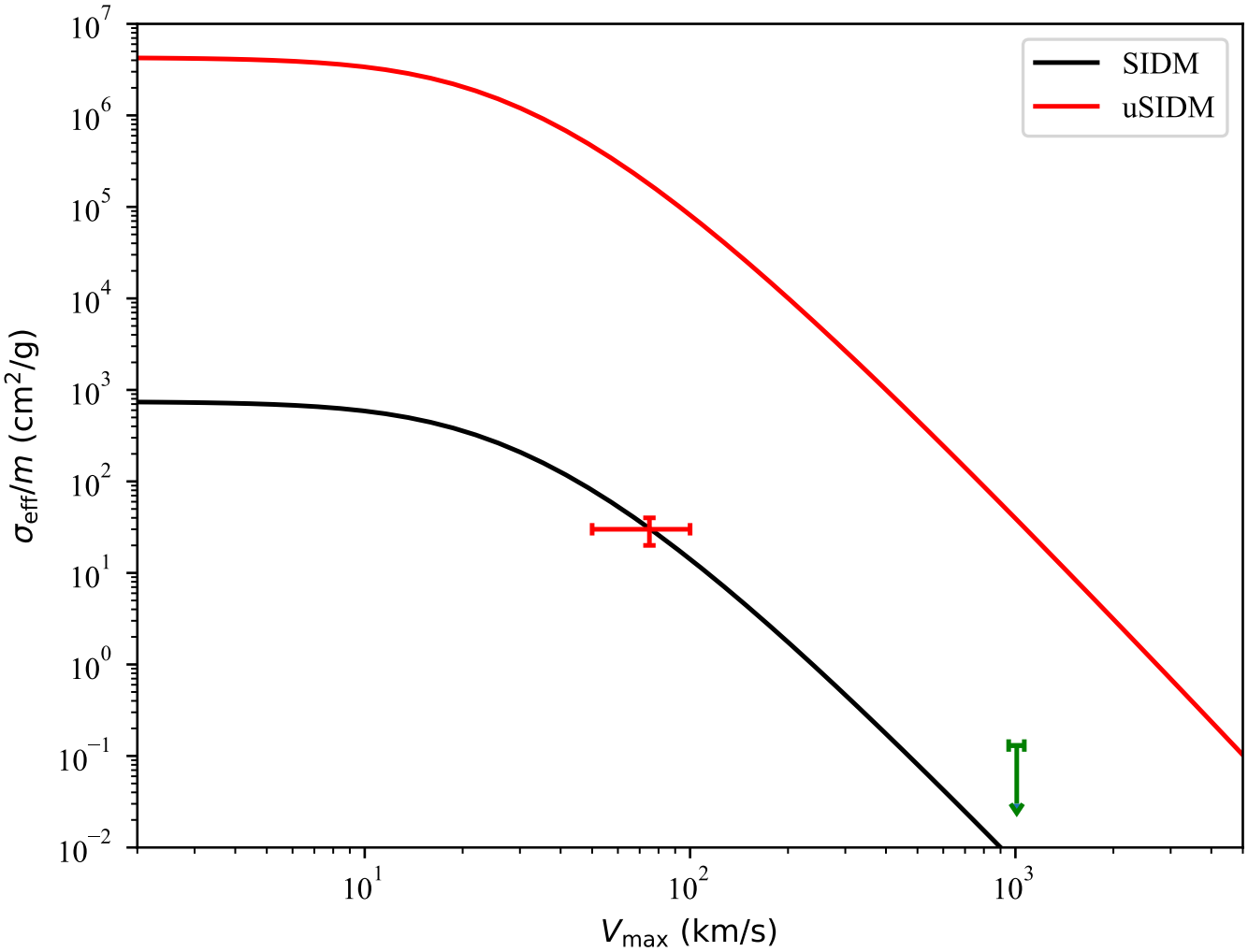

Figure: Using the relic density parameters (the orange curve)

Gravothermal Evolution and Core Collapse

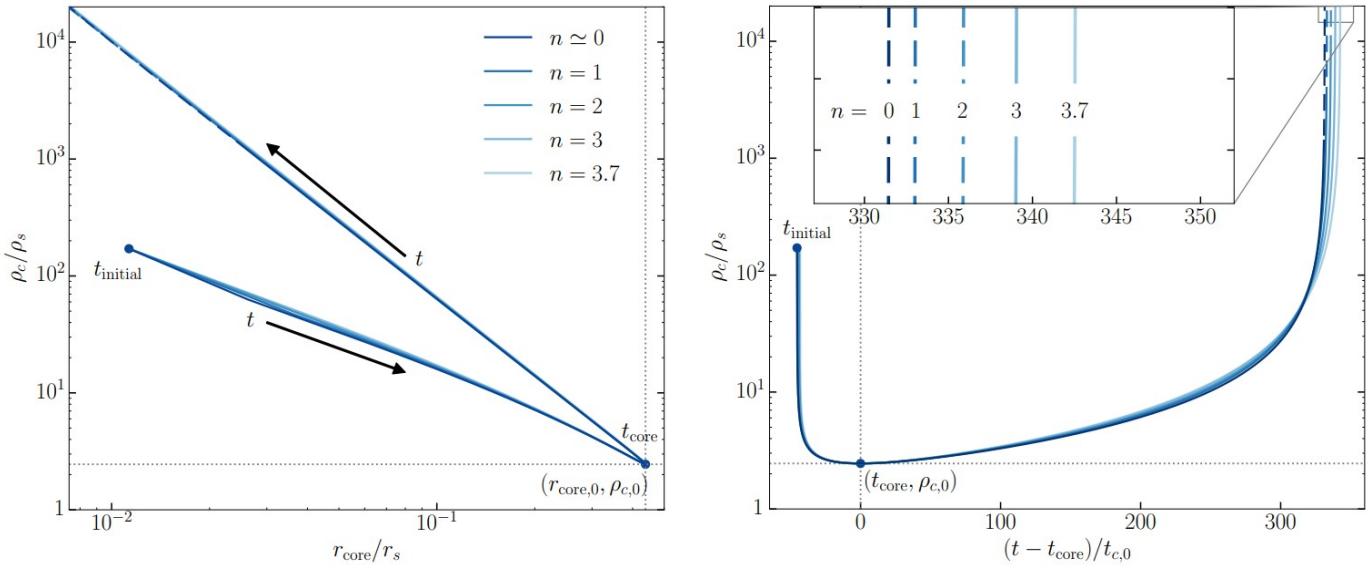

Figure: From Outmezguine 2023, arXiv:2204.06568, fit to fluid sims

Physically, the self interactions of the dark matter causes heat to flow outwards from the core, which grows the core - until a brief equilibrium is reached; upon which the process reverses and the core begins to shrink

While the above theory curves are very helpful, here is a plot that shows how this physically changes the dark matter density profile:

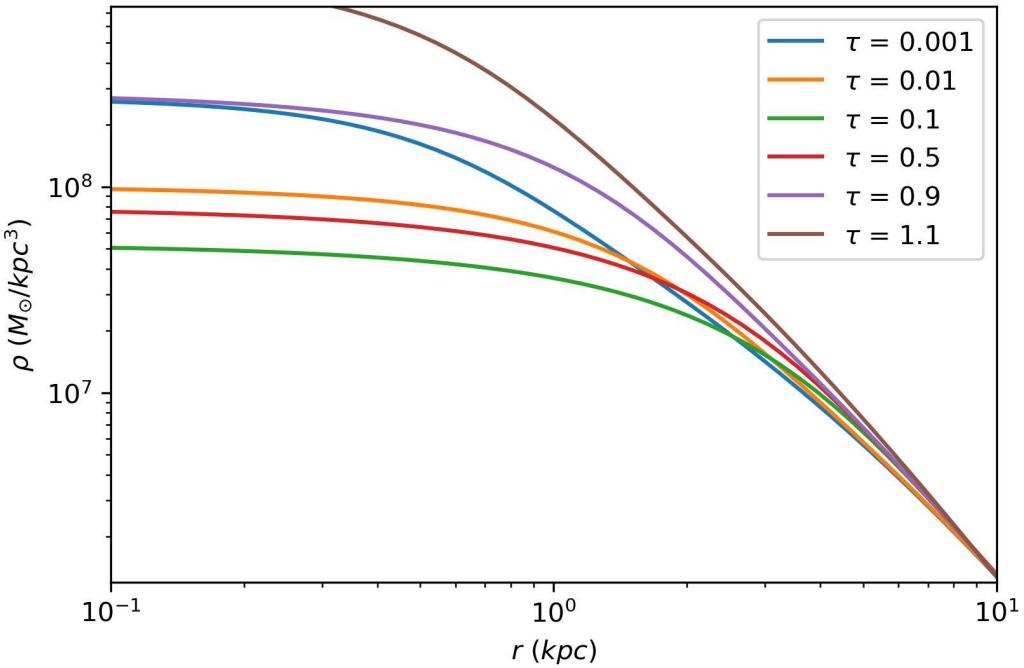

τ is a dimensionless time parameter which I will explain in more detail later, but $\tau = 0$ is the initial starting configuration for the halo

Data Set:

From the SPARC data set, we chose 10 galaxies: DDO 154, ESO 444-G084, F568-V1, F574-1, NGC 0300, NGC 3109, UGC 00128, UGC 06446, UGC 06667, and UGC 08286

From the Relatores et al 2019 data set, we chose 4 galaxies: NGC 4376, NGC 4396, NGC 7320, and UGC 4169

The criteria for our chosen galaxies was that they needed to all be similarish in V_{max}, and that they needed to be dark matter dominated at their innermost measured data point, typically $r < 0.5 - 1$ kpc for SPARC, but $r \leq 0.5$ kpc for Relatores

Galaxy Rotation Curves

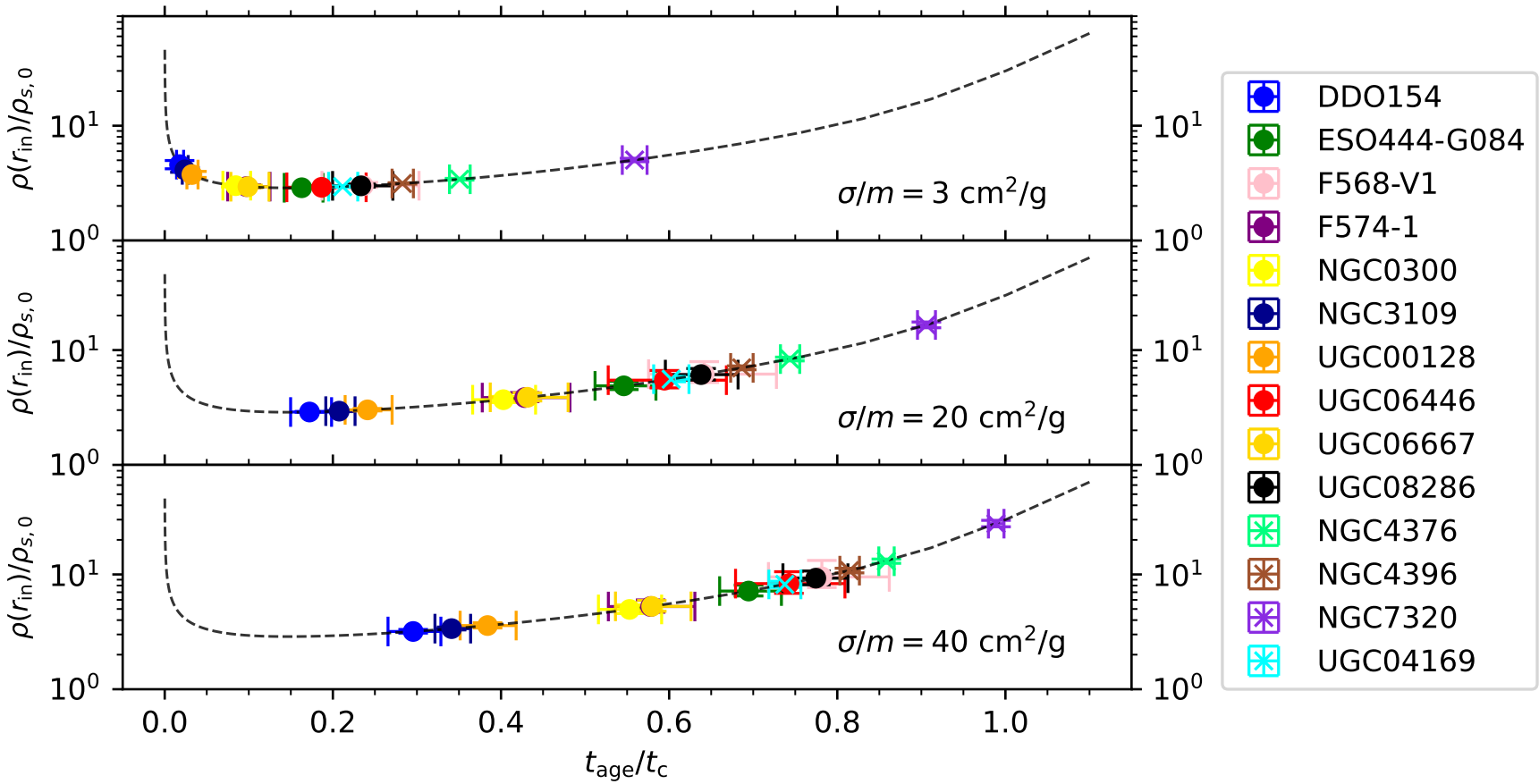

Figure: Fits from Roberts et al 2024, arXiv:2407.15005

Galaxy Rotation Curves Particle Physics

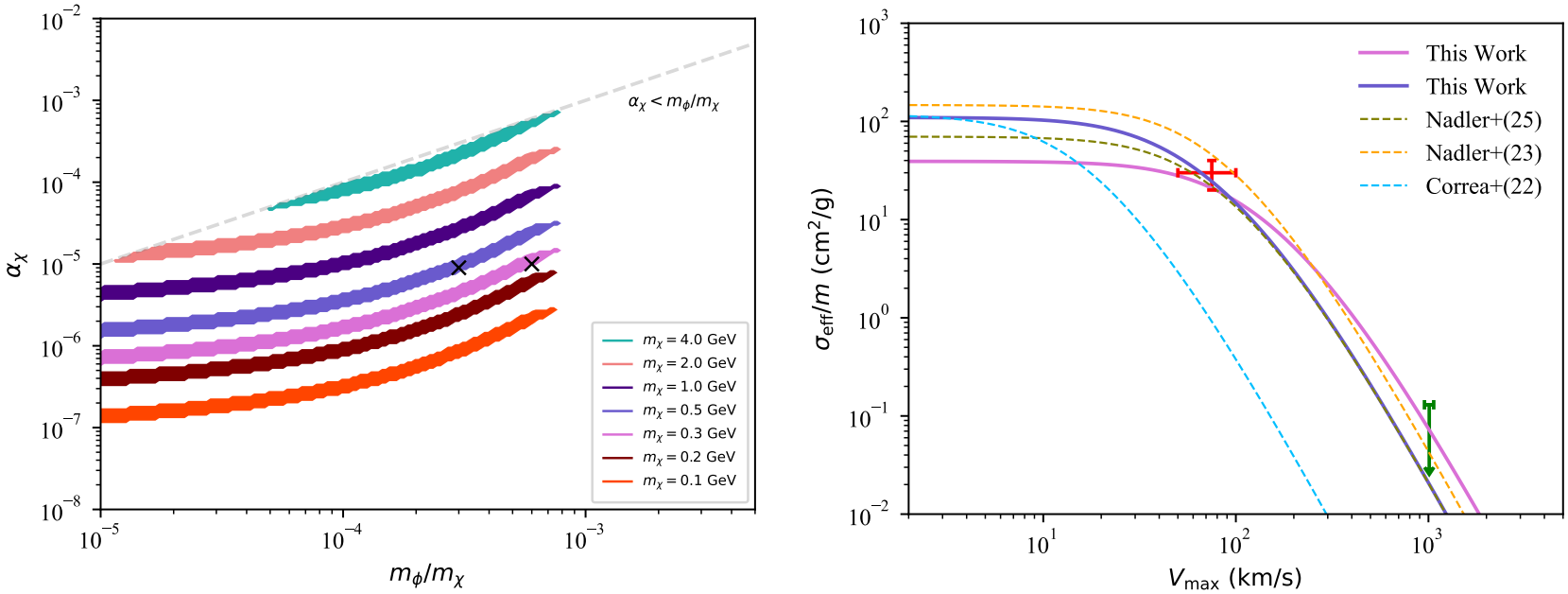

Figure: Left panel: Favored parameter regions where the effective SIDM cross section satisfies the following conditions simultaneously: $\sigma_{\rm eff}/m = 20$–40 cm^2/g at $V_{\rm max} = (75 \pm 25)$ km/s, and $\sigma_{\rm eff}/m < 0.13$ cm^2/g at $V_{\rm max} = (1000 \pm 55)$ km/s. Right panel: Effective cross sections as a function of $V_{\rm max}$ for the cases $m_\chi = 0.3$ GeV (pink) and 0.5 GeV (purple).

Backup Slide: Seeding SMBHs via uSIDM

Instabilities of metal-poor gas clouds

These clouds are unstable enough to allow for collapse into a BH rather than fragmentation into forming stars first. While these directly form BHs, the mass range is $m_{\rm BH}^{\rm seed} \approx 10^4\ {\rm M}_\odot$, which requires long phases of Eddington or super-Eddington accretion, and as we just discussed, has several problems

Stellar-dynamical methods

As early primordial gas becomes enriched with heavy elements via Pop III stars, the next generation of stars form. If there is a sufficiently dense population of low mass stars, they can form nuclear star clusters where runaway stellar mergers grow the stars into large enough objects that then collapse into BHs with $m_{\rm BH}^{\rm seed} \approx 10^2 - 10^4\ {\rm M}_\odot$. Unfortunately, as the metallicity of the gas increases, this process becomes less efficient

Backup Slide: Seeding SMBHs via uSIDM

Mergers

While simulations have shown that mergers are the primary mechanism of growth for high redshift BHs, this is high dependent on the formation of heavy seeds and their distributions. However, velocity kicks can slingshot one of the merging BHs out of the system entirely, hence ending the growth cycle of the primary BH seed. The merger process also may not occur fast enough to match observations

$\longrightarrow$ Because of these issues, we elected to explore the possibility of gravothermally collapsing dark matter halos into SMBH seeds much earlier, which can then grow via accretion within the observational limits

First, we compute the collapse redshift, $z_{\rm coll}$, for forming the BH seed from gravothermal collapse of the halo:

$$t(z_{\rm coll}) - t(z_{\rm vir}) = 455.65\ t_{\rm rel}\left(f, \sigma/m, m_{200}, z_{\rm vir}, c_{200}\right), \qquad (1)$$

where the relax time, $t_{\rm rel}$, is defined as

$$t_{\rm rel}\left(f, \sigma/m, m_{200}, z, c_{200}\right) = 0.354\,{\rm Myr}\left(\frac{m_{200}}{10^{12}\,{\rm M}_\odot}\right)^{-1/3}\left(\frac{k_c(c_{200})}{k_c(9)}\right)^{3/2} \times \left(\frac{c_{200}}{9}\right)^{-7/2}\left(\frac{\rho_{\rm crit}(z)}{\rho_{\rm crit}(z=15)}\right)^{-7/6}\left(\frac{f\sigma/m}{1\ {\rm cm}^2/{\rm g}}\right)^{-1}, \qquad (2)$$

with $k_c(x) = \ln(1+x) - x/(1+x)$ and $\rho_{\rm crit}(z)$ the critical density of the universe at a given redshift.

The time is given in the typical way,

$$t(z) = \int_z^\infty \frac{dz'}{(1+z')H(z')}, \tag{3}$$

with $H(z)$, the Hubble rate. From Pollack et al 2015, they ran simulated halos to infer how much of the inner core would fully collapse into the BH seed, they found that a typical amount of about 2.5% of m_{200} would turn into the seed, which sets the normalization for their estimate of the BH seed formation mass:

$$\frac{m_{\rm BH}(z)}{m_{200}} \sim \frac{0.025 f}{\ln(1+c_{200}) - \frac{c_{200}}{1+c_{200}}}. \tag{4}$$

Seeding SMBHs via uSIDM

Once the seed has formed, we grow the seed via accretion to an observed quasar redshift,$z_{\rm obs}$. We control the accretion rate by parameterizing it to the number of number of e-folds of accretion (N_e) during which the SMBH grows, as:

$$t(z_{\rm obs}) = t(z_{\rm coll}) + N_e t_{\rm sal}, \tag{5}$$

where $t_{\rm sal}$ is the Salpeter time; which is the time scale it would take a BH to double its mass via Eddington accretion and is given by,

$$t_{\rm sal} = \frac{\epsilon_r \sigma_T c}{4\pi G m_p} \approx \left(\frac{\epsilon_r}{0.1}\right) 45.1 \text{ Myr}. \tag{6}$$

Following the literature, we set $\epsilon_r = 0.1$. The seed then grows exponentially as: $m_{\rm BH}^{\rm theory}(z_{\rm obs}) = m_{\rm BH}^{\rm seed}(z_{\rm coll}) \exp(N_e)$.

Backup Slide: Seeding SMBHs via uSIDM

The full 8 quasar sample:

Quasar	$\log_{10} M_\bullet\ (M_\odot)$	z
J0100+2802	10.29	6.327
	10.09	6.316
	10.33	6.300
J0842+1218	9.404	6.075
	9.300	6.067
	9.520	6.070
	9.230	6.069
P007+04	9.356	6.002
	9.890	5.954
	9.910	5.980
P036+03	9.775	6.541
	9.430	6.527
P183+05	9.674	6.439
	9.410	6.428
P231-20	9.806	6.587
	9.520	6.564
P323+12	9.243	6.587
	8.920	6.000
P359-06	9.577	6.172
	9.000	6.169

Backup Slide: uSIDM Power-law fit

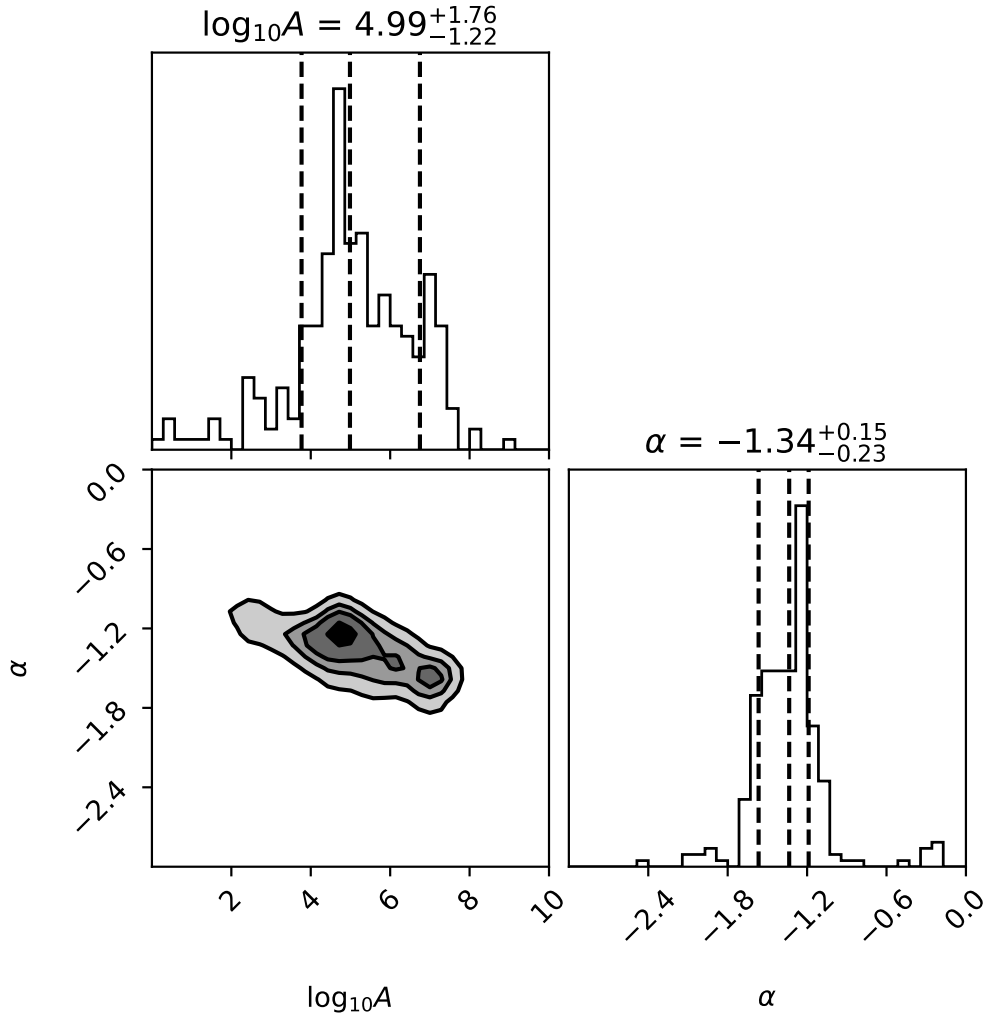

Figure: Power-law fit: $\frac{dN_{BH}}{d\log_{10} m_{\rm BH}} = A\, m_{\rm BH}^{\alpha}$

uSIDM Observables: Transfer Function

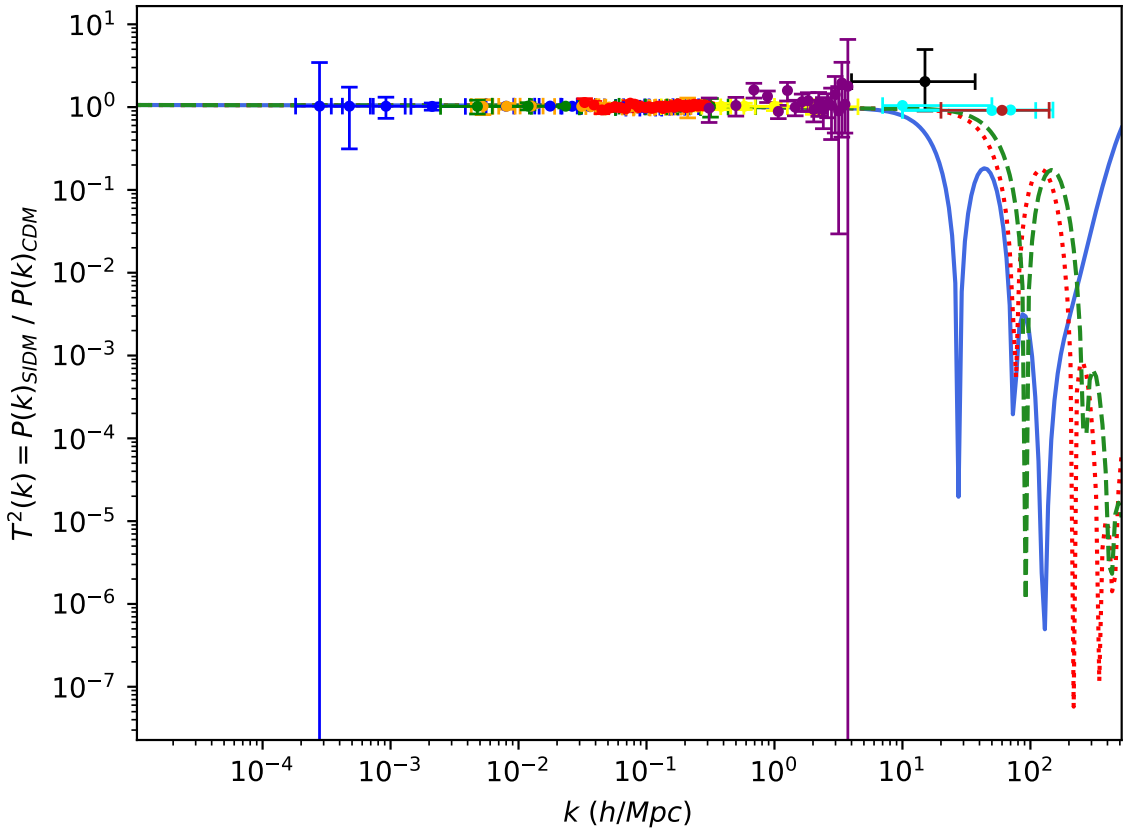

LRD SED

They have an interesting property of a “v-shaped” spectral energy distribution. The top is from Kokorev et al 2024 arXiv:2401.09981 and bottom is from Zhang et al 2025 arXiv:2505.12719

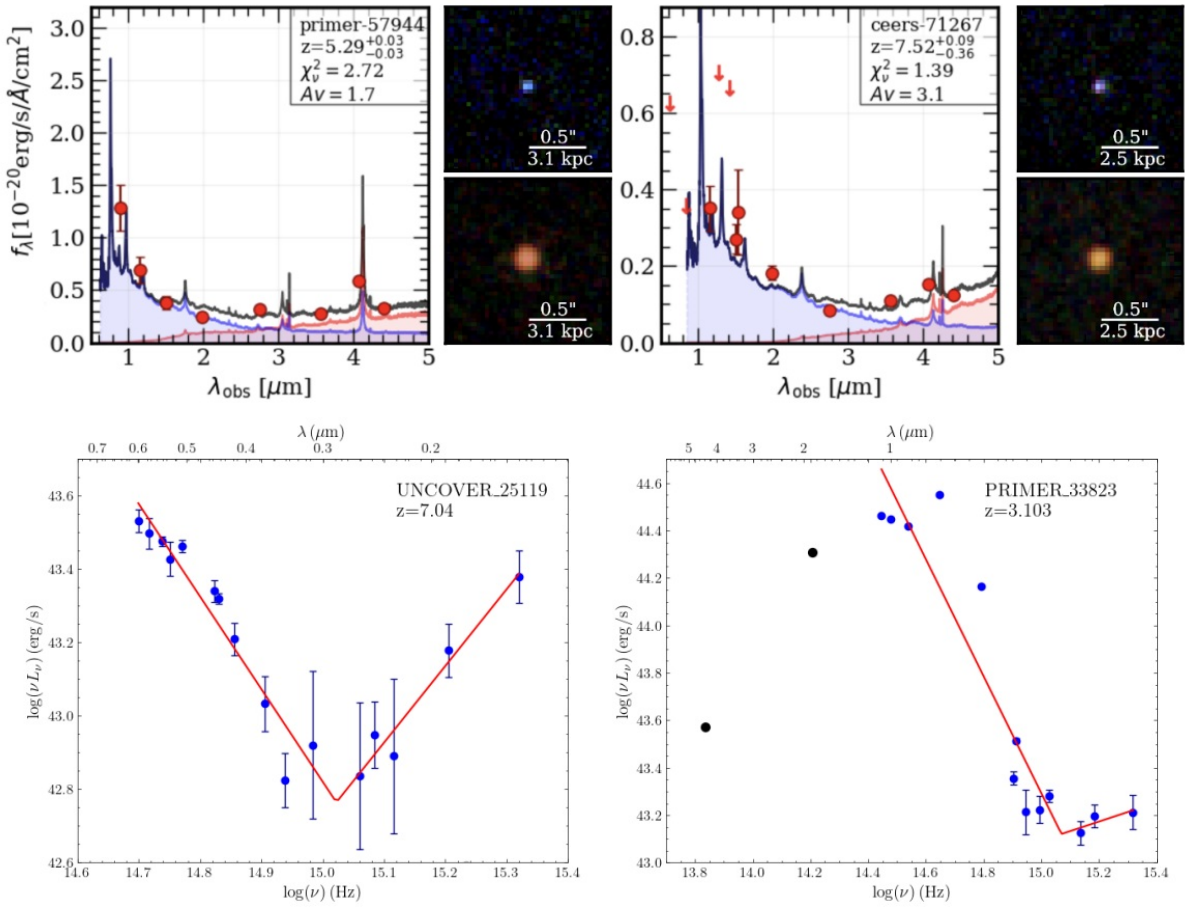

$$\sigma_V = \frac{3}{2}\int d\cos\theta \sin^2\theta \frac{d\sigma}{d\cos\theta} \tag{7}$$

$$\frac{d\sigma}{d\cos\theta} = \frac{\sigma_0 w^4}{2\left[w^2 + v^2\sin^2\left(\theta/2\right)\right]^2} \tag{8}$$

$$\sigma_V = \frac{6\sigma_0 w^6}{v^6}\left[\left(2+\frac{v^2}{w^2}\right)\ln\left(1+\frac{v^2}{w^2}\right) - \frac{2v^2}{w^2}\right] \tag{9}$$

$$\sigma_{\text{eff}} = \frac{2\int v^2 dv\ d\cos\theta \frac{d\sigma}{d\cos\theta} v^5 \sin^2\theta\ \exp\left[-\frac{v^2}{4(\sigma_{1\text{D}})^2}\right]}{\int v^2 dv\ d\cos\theta v^5 \sin^2\theta\ \exp\left[-\frac{v^2}{4(\sigma_{1\text{D}})^2}\right]} \tag{10}$$

$$\sigma_{\text{eff}} \approx \frac{1}{512\left(\sigma_{1\text{D}}\right)^8}\int v^2 dv\ \frac{2}{3}\sigma_V v^5\ \exp\left[-\frac{v^2}{4\left(\sigma_{1\text{D}}\right)^2}\right] \tag{11}$$

where $\sigma_0 = 4\pi\alpha_\chi^2/\left(m_\chi^2 w^4\right)$ and $w = m_\phi c/m_\chi$